

1'

# Initial Galileo Gravity Results and the Internal Structure of Io

J. D. Anderson and W. L. Sjogren

Jet Propulsion Laboratory

California Institute of Technology

Pasadena, California 91109-8099

G. Schubert

Department of Earth and Space Sciences

Institute of Geophysics and Planetary Physics

University of California

Los Angeles, California 90095-1567

March 5, 1996

Correspondence and Proofs to:

Dr. John D. Anderson

MailStop 301-230

Jet Propulsion laboratory

California Institute of Technology

Pasadena, CA 91109--8099

Phone: (818) 354-3956

Fax: (818) 393-0028

E-Mail: [john.d.anderson@jpl.nasa.gov](mailto:john.d.anderson@jpl.nasa.gov)

#### Author Note

This article contains results from the Galileo spacecraft's arrival at Jupiter on December 7, 1995. We report the discovery of a tri-axial gravity field for the innermost Galilean satellite 10. Based on this discovery, we conclude that 10 has a large metallic core. If the core is a eutectic mixture of iron and iron sulfide, it most likely comprises 20.2 percent of 10's mass and extends to 52 percent of its mean radius (1 821.3 km).

## ABSTRACT

Using the Galileo spacecraft's 2.3 GHz (13 cm) transmitted carrier wave, the National Aeronautics and Space Administration's Deep Space Network generated radio Doppler data around the time of Jupiter arrival, including the 10 flyby on 7 December, 1995. Near the time of Io's closest approach at an altitude of 897 km, these data reveal a clearly detectable gravity signal. The signal's source is a tri-axial gravity field characterized by spherical harmonics  $J_2$  and  $C_{22}$ . Our measured value of  $C_{22}$  exceeds the expected nonhydrostatic value by a factor of 25 or more. Therefore, it provides a useful boundary condition on interior models. Assuming that Io is a body in tidal and rotational equilibrium, we conclude it has a large metallic core. If the core is a eutectic mixture of iron and iron sulfide (Fe-FeS core), it comprises  $20.2 \pm 7.4$  percent of Io's total mass ( $8.932 \times 10^{22}$  kg). Alternatively, if the core is pure iron (Fe core), it comprises  $10.5 \pm 3.75$  percent of the total mass. The corresponding radius for the Fe-FeS core is  $942 \pm 118$  km, or about 52 percent of Io's mean radius (1821.3 km). The radius for the alternate Fe core is  $651 \pm 79$  km, or about 36 percent of the mean radius. We also report improved masses for Io, Europa, and Jupiter. The new mean densities for Io and Europa are  $3529.44 \pm 1.3$  and  $2984 \pm 46$  kg m<sup>-3</sup>, respectively.

## 1 Introduction

Io is arguably the most bizarre object in the solar system - - at least it is the most volcanic. It is covered by flows of sulfur, sulfur compounds, and silicates. Its mean density of  $3529$  kg m<sup>-3</sup> and rugged topography suggest an interior comprised of silicates, similar to the interiors of the Earth and the Moon, as well as heavier metals (1). Io's proximity to Jupiter, almost

318 times more massive than Earth, distinguishes it from the Moon, though Io and the Moon are similar in some respects (2). However, forces producing a rotational distortion are 220 times larger on Io than on the Moon. Furthermore, Io's tidal distortions are comparable in magnitude to its rotational distortions (3).

Assuming Io is a body in tidal and rotational equilibrium, we are justified in concentrating the gravity analysis on two hydrostatic gravity coefficients,  $J_2$  and  $C_{22}$  (4). If the nonhydrostatic  $C_{22}$  is comparable to that of the Moon ( $C_{22} = 22.3 \times 10^{-6}$ ), it is just about at the limit of detectability with the Galileo flyby. Because the flyby gravity signal is about 25 times larger (Fig. 1), it represents a detection of the hydrostatic component. For the nonhydrostatic Moon, the dimensionless and scaled moment of inertia  $C/MR^2 = 0.3904$  is determined from a combination of the Moon's gravity field and physical librations ( $C$  is the moment of inertia about the rotation axis). However, for Io, the moment of inertia is determined by Radau-Darwin equilibrium theory alone (5). This derived moment of inertia provides an important constraint on the degree of central condensation in the interior. For a sphere of constant density,  $C/MR^2 = 2/5$ , so any value of  $C/MR^2$  significantly smaller implies some degree of central condensation.

## 2 Data

The Galileo spacecraft's telecommunication system is limited by the loss of a high-gain antenna that failed to unfurl before Jupiter arrival (6). During Io flyby, radio signals at S band (2.3 GHz or 13 cm wavelength) were transmitted to Earth using a low-gain antenna and a temperature-controlled crystal oscillator (USO) for frequency reference. The Deep Space

Network (DSN) compensated for the low signal to noise ratio by using recently developed low- noise digital receivers (Block V). Also, they tracked the spacecraft with their largest 70 meter antennas in California, Australia, and Spain. Besides extracting engineering and science telemetry, they generated Doppler data from the carrier wave. These radio Doppler data, in a format of discretely sampled cycle count, were electronically delivered to the Galileo Project's Navigation Team, who in turn made them available to us. We have placed the data in the public domain by transferring all data files used in our analysis to 9-track magnetic tape, and by sending copies to the National Space Science Data Center, Goddard Space Flight Center. Any further permanent archiving of the data will be accomplished by the National Aeronautics and Space Administration's Planetary Data System.

Because the USO is temperature controlled, it is subject to a minimum of environmental effects. However, crystal oscillators are inherently less stable than atomic frequency standards. Hence, the DSN sometimes generates phase-coherent Doppler data using the spacecraft's transponder and the DSN's three 70-meter stations referenced to hydrogen masers. We have included Doppler measurements generated outside critical periods surrounding Io flyby. The coherent data, although generated when the spacecraft was too far from Io to reveal a gravity signal, nevertheless provide a stable baseline for the USO data. Also, by providing information on the Io flyby orbit, they free the USO data for the gravity-field determination.

The data used in our analysis start with coherent Doppler at 4 December 1995, 01:52:13 (all times are Universal Time Coordinated, UTC, at Earth reception of the Galileo signal), and end with USO data at 7 December 1995, 20:59:30, about two hours before the start of relay data from the Galileo Atmospheric Probe (7). The Doppler starting time is early

enough to assure a good orbit determination during 10 flyby (closest approach at 18:38:00). Two criteria determined the ending time. First, the data ended before a propulsion burn at about 8 December 01:19. This burn inserted the spacecraft into the desired Jupiter orbit. inclusion of data during the propulsion maneuver would have introduced troublesome non-gravitational forces on the spacecraft motion. Second, although the USO was relatively immune to environmental effects, it experienced a significant shift in frequency as the radiation dose from Jupiter's magnetospheric particles increased. Any USO data taken after the selected ending time would have seriously biased the orbit determination, and consequently the gravity results.

The reduced data for the experiment are Doppler frequency data. Frequency data are defined as the difference in cycle count at two times divided by the time interval. Most of the reduced frequency data are sampled at 60 s, but near 10 closest approach, for an interval of about two hours, the USO data are sampled at 10 s. This sampling strategy suppresses the high-frequency Fourier noise components (low-pass filter), and, in addition, it assures adequate resolution of the gravity signal during flyby.

### 3 Data Analysis

We used the Orbit Determination Program (ODP) of the Jet Propulsion Laboratory (JPL) to fit the radio Doppler data by nonlinear weighted least squares (8). The one-sigma error on each Doppler velocity measurement was assumed equal to  $2 \text{ mm s}^{-1}$  for both USO data and coherent Doppler data sampled at 60 s. For the two hours of USO data sampled at 10 s, the one-sigma error was increased by the square root of six. An ODP algorithm,

applied automatically, increased the Doppler error at lower elevation angles with respect to the station's horizon.

A total of 23 parameters were adjusted to find the local minimum of the weighted residuals. The nonlinear process successfully converged. The parameters consisted of the six cartesian position and velocity coordinates of the spacecraft; six similar cartesian coordinates for Io's ephemeris (orbit); three GM values for, respectively, the Jupiter system, Io, and Europa; the 10 gravity coefficients  $J_2$  and  $C_{22}$ ; and six polynomial coefficients that fit the drift in the spacecraft oscillator (USO) by two quadratic polynomials (spacecraft time as independent variable). Both the spacecraft orbit and the Io orbit were numerically integrated at each iteration in the nonlinear process. All other dynamical and geodetic parameters were fixed at currently accepted values (9). The orbits and station coordinates were referenced to the J2000 system using the latest JPL Lunar and Planetary Development Ephemeris (DE403). Models for the Earth's polar motion and nonuniform rotation were provided by the DSN.

All 10 gravity coefficients except  $J_2$  and  $C_{22}$  were fixed at zero, a reasonable assumption given their expected size. The coefficient  $J_2$  could not be determined independently of Io's GM and  $C_{22}$ , so we imposed the hydrostatic constraint that  $J_2$  is exactly 10/3 of  $C_{22}$ . The adjustment of Europa's mass was an afterthought, only included when we saw a clear signal in the USO Doppler residuals near Europa closest approach. The removal of this signal required a reduction in the Europa mass determined by Pioneer and Voyager flybys by 0.19 percent, consistent with its prior error of 0.38 percent (10).

Obviously, not all components of Io's ephemeris could be determined from a single flyby, so we introduced prior information (n-dimensional Bayesian statistics) in the form of a covari-

ance matrix determined from ground-based observations (11). The Galileo radio Doppler data increased Io's orbital radius by  $9.64 \pm 4.2$  km, while the adjustment to orbital velocity of  $-3963 \pm 130$  mm s<sup>-1</sup> left Io's total orbital energy and orbital angular momentum unaffected. A change in orbital energy would have changed Io's orbital period, and hence would have been inconsistent with long-term astrometric observations. Similarly, a significant change to angular momentum would have produced an unacceptably large change to orbital eccentricity. We avoided such inconsistencies by using integrated satellite ephemerides and their associated covariance matrix as a priori information (12). In terms of osculating elements at the ODP epoch, the increase in orbital radius produced a correction of  $0.07472^\circ$  to Io's osculating true anomaly. The orbit's longitude was unaffected, however, so the positive change in true anomaly was offset by a corresponding negative change in the longitude of Io's perijove location (13).

The two quadratic polynomials for the USO drift were assumed independent. The first started at the ODP epoch of 4 December 01:52:02 UTC and ended 16 minutes after 10 clocks approach. This polynomial revealed a decrease in the USO frequency by 46 mHz over the 89 hour interval. At S band (2.3 GHz) this amounted to a change in fractional frequency  $\Delta\nu/\nu$  of  $1.6 \times 10^{-11}$  well within the limits of plausibility for an inherent random walk in the crystal's frequency (6). The 01:11' is fully relativistic, so the gravitational redshift was accounted for. The second polynomial started where the first one stopped, and continued for about two hours to the last Doppler measurement in the fit. We extended the fit this far because the frequency drift was sufficiently linear. The USO frequency increased by 660 mHz ( $\Delta\nu/\nu \approx 2.9 \times 10^{-10}$ ) over the last two hours, most assuredly a result of radiation dose to the crystal.



The Io flyby at  $15.0 \text{ km s}^{-1}$  at an altitude of 897 km, and nearly in Io's equatorial plane (closest approach at latitude  $-8.5^\circ$  and west longitude 101.10), yielded the new result  $C_{22} = (559 \pm 27) \times 10^{-6}$ . Io's GM was improved to  $5959.91 \pm 0.28 \text{ km}^3 \text{ s}^{-2}$ . In the same units, the GM for the Jupiter system was improved to  $126,712,752 \pm 40$ , and the flyby of Europa at a distance of 32,958 km at 14:00:54 UTC (Earth time) yielded a GM of  $3196.81 \pm 0.69$  (14). This and other gravity constants determined so far by the Galileo Mission are listed in Table 1. A comparison to prior Pioneer and Voyager results is included as well (10).

Masses derived from the GM determinations depend on knowing the gravitational constant  $G$ . The currently accepted value is  $(6.67259 \pm 0.00085) \times 10^{-20} \text{ km}^3 \text{ s}^{-2} \text{ kg}^{-1}$  (15). This yields a mass of  $(8.9319 \pm 0.0012) \times 10^{22} \text{ kg}$  for Io and  $(4.7910 \pm 0.0012) \times 10^{22} \text{ kg}$  for Europa. The Jupiter GM is obtained by subtracting the four Galilean satellite masses from the system mass. The Pioneer and Voyager values for Ganymede and Callisto are  $9887 \pm 3$  and  $7181 \pm 3 \text{ km}^3 \text{ s}^{-2}$ , respectively (10). The corresponding Jupiter GM is  $126,686,527 \pm 40 \text{ km}^3 \text{ s}^{-2}$  and its mass is  $(1.89861 \pm 0.00024) \times 10^{27} \text{ kg}$ . The ratio of the mass of the Sun to the mass of the entire Jupiter system is  $1047.34873 \pm 0.00033$  (16).

## 4 Geophysical Discussion

A synchronously rotating satellite in tidal and rotational equilibrium takes the shape of a tri-axial ellipsoid with dimensions  $a, b, c$  ( $a > b > c$ ). The long axis of the ellipsoid is along the planet-satellite line and the short axis is parallel to the rotation axis. The distortion of the satellite depends on the magnitude of the rotational and tidal forcing and the distribution of mass with radius inside the body. The distortion of the satellite and its internal mass

distribution find expression in the satellite's gravitational field. Accordingly, knowledge of the gravitational field, for example the value of  $C_{22}$ , can be used to infer the nature of the satellite's internal mass distribution (5).

The gravitational coefficient  $C_{22}$  is related to the difference in the equatorial moments of inertia by

$$C_{22} = \frac{B - A}{4MR^2} \quad (1)$$

where the ellipsoidal satellite's principal moments of inertia are  $A, B, C$ , ( $C > B > A$ ). For a body in rotational and tidal equilibrium, the gravity coefficient  $C_{22}$  is related to the rotational response parameter  $q_r = 1.7123 \times 10^{-3}$  (2) by

$$C_{22} = \frac{3}{4} \alpha q_r \quad (2)$$

where  $\alpha$  is a dimensionless response coefficient that depends on the distribution of mass within the satellite ( $\alpha = 1/2$  for constant density). Given  $C_{22}$ , (2) determines  $\alpha$ , and the satellite's axial moment of inertia  $C$  follows from

$$\frac{C}{MR^2} = \frac{2}{3} \left[ 1 - \frac{2}{5} \left( \frac{4 - 3\alpha}{1 + 3\alpha} \right)^{1/2} \right] \quad (3)$$

The Doppler data analysis yields  $\alpha = 0.435$  and  $C/MR^2 = 0.378$  for the nominal value of  $C_{22} = 559 \times 10^{-6}$ .

The axial moment of inertia leads directly to the internal mass distribution but it requires a model of the interior. Consistent with the constraint on the internal mass distribution in-ovided by the single datum  $C_{22}$ , we assume a simple two-layer model for 10 consisting of a core of radius  $r_c$  and density  $\rho_c$  surrounded by a mantle of density  $\rho_m$ . The mean density  $\bar{\rho}$  of the two-layer model is

$$\bar{\rho} = \frac{r_c^3}{R^3} (\rho_c - \rho_m) + \rho_m \quad (4)$$

and the axial moment of inertia of the two layer model is

$$\frac{C}{MR^2} = \frac{2}{5} \left[ \frac{\rho_m}{\bar{\rho}} + \left( 1 - \frac{\rho_m}{\bar{\rho}} \right) \left( \frac{r_c}{R} \right)^2 \right] \quad (5)$$

In this representation, the core density  $\rho_c$  and radius  $r_c$  are the basic unknowns of the two-layer model. For an assumed value of  $\rho_c/\bar{\rho}$ , (4) yields  $\rho_m/\bar{\rho}$  in terms of  $r_c/R$ . Then, (5) yields the fractional core radius  $r_c/R$ . Basically, three unknown parameters,  $\rho_c$ ,  $r_c$ , and  $\rho_m$ , fully describe the two-layer model. We assume a value for  $\rho_c$  and determine the other two parameters from the known mass and inferred moment of inertia.

We summarize results in Table 2 for assumed core densities of 5150 and 8090 kg m<sup>-3</sup>, reasonable values for Fe-FeS and Fe cores in 10 (17). The three values of  $C_{22}$  are the inferred value of  $C_{22}$  from the Doppler data and its plus and minus one-sigma variations. Hence, the central column of numbers is the most likely. The core radius in these models is between about 45% and 58% of Io's radius if the core is FeFeS, and between about 31 % and 40% if the core is Fe., The mass of the core is between about 13% and 28% of Io's mass, for an FeFeS core composition, and between about 7% and 14% for a pure iron core. Uncertainty in the actual value of  $\rho_c/\bar{\rho}$  results in the possible values of core size and mass shown in Fig. 3.

The theory for the equilibrium distortion of 10 allows determination of the ellipsoidal shape of these models, so values of  $(a-c)/c$  and  $(b-c)/c$  are also included in Table 2. These values are independent of the choice of  $\rho_c/\bar{\rho}$ ; they compare well with the determination of Io's shape from Voyager 1 imaging data (18).

Though lack of knowledge of the chemical composition of 10's core precludes us from deriving the exact size and mass, the conclusion that Io has a large metallic core is robust.

The gravitational signal of this core has been unambiguously detected during the Galileo flyby of Io. In comparison, there is yet no certain observational detection of a lunar core, which is at most about 20% of the Moon's radius.

## 5 References and Notes

1. For a description of Io and other Jupiter satellites see D. Morrison, Ed., *Satellites of Jupiter* (Univ. of Arizona Press, Tucson, 1982) and J. A. Burns and M. S. Matthews, Eds., *Satellites* (Univ. of Arizona Press, Tucson, 1986).
2. For example, Io's mean radius is 1821.3 km, roughly five percent larger than the Moon's 1738 km radius; Io's mean density of  $3529 \text{ kg m}^{-3}$  is somewhat larger than the Moon's  $3344 \text{ kg m}^{-3}$  density; its average surface gravitational acceleration  $g$  is  $1.798 \text{ m s}^{-2}$  compared to a lunar  $g$  of  $1.601 \text{ m s}^{-2}$ ; like the Moon, it is in synchronous rotation with its orbital period. It differs most significantly in its sidereal rotational period of 1.769 days versus 27.3217 days for the Moon. The rotational response parameter  $q_r = \omega^2 R^3 / GM$ , the ratio of centrifugal to gravitational acceleration at the equator, is  $1.7123 \times 10^{-3}$  for Io, while for the Moon it is  $7.757 \times 10^{-6}$ . Here  $\omega$  is the satellite's angular rotation rate,  $R$  is its mean radius,  $M$  is its mass, and  $G$  is the gravitational constant.
3. B. O'Leary, T. C. Van Flandern, *Icarus* 17, 209-215 (1972).
4. For the standard spherical harmonic representation of the gravitational potential see for example, W. M. Kaula, *Theory of Satellite Geodesy* (Blaisdell, Waltham, MA, 1966). The coefficients  $J_2$  and  $C_{22}$  give the contributions to the gravitational potential

of the spherical harmonics of degree  $\ell$  and order  $m$  for  $\ell = 2, m = 0$  and  $\ell = 2, m = 2$ , respectively.

5. 'There is an extensive literature on the necessary theory. For example, W. M. Kaula, *An Introduction to Planetary Physics: the Terrestrial Planets* (Wiley, New York, 1968), W. B. Hubbard and J. D. Anderson, *Icarus* 33, 336-341 (1978), S. F. Dermott, *Icarus* 37, 310-321 (1979), V. N. Zharkov, V. V. Leontjev, A. V. Kozenko, *Icarus* 61, 92-100 (1985), all discuss the theory from different perspectives.
6. J. D. Anderson *et al.*, *Space Sci. Rev.* 60, 591-610 (1992) give a description of the Galileo gravitational experiments for all phases of the mission. The radio propagation experiments and a description of radio instrumentation and measurement techniques are discussed by H. T. Howard *et al.*, *Space Sci. Rev.* 60, 565-590 (1992). The main spacecraft antenna that failed to unfurl is a 4.8 m paraboloid attached to the spinning portion of the spacecraft and aligned with the axis of rotation. The crystal oscillator, called the Ultra-stable Oscillator (USO) by JPL, is a spare from the Voyager Mission. It is typical of temperature-controlled flight units of the mid 1970's. For Doppler integration times  $\tau$  less than one second, its frequency is dominated by white phase noise. Between  $\tau = 1$  and 300 s, the frequency noise is white with a  $\Delta\nu/\nu$  standard error of  $10^{-12}$ . For Doppler integration times greater than 300 s, the frequency random walks such that the frequency error is proportional to  $\tau^{1/2}$  - consistent with our data analysis. Current USO technology is far superior. USO specifications for the Cassini Saturn Mission, due for launch in late 1997, include a goal for fractional frequency error of  $2 \times 10^{-14}$  at  $\tau = 1000$  s.

7. An overview of the Galileo Mission, including a description of the spacecraft configuration (Orbiter and Probe), is given by 'P. V. Johnson and C. M. Yeats, *Space Sci. Rev.* 60,3-21 (1992).
8. The ODP uses nonlinear weighted least squares, called chi-squared fitting with nonlinear models by W. H. Press, S. A. Teukolsky, W. T. Vetterling, B. P. Flannery, *Numerical Recipes* (Cambridge Univ. Press, Cambridge and New York, ed. 2, 1992). The specific problem of fitting radio Doppler data to spacecraft trajectory models is discussed by T. D. Moyer, *Technical Report No. TR 32-1527* (Jet Propulsion Laboratory, Pasadena, 1971) and J. D. Anderson, in *Experimental Gravitation*, B. Bertotti, Ed. (Academic Press, New York and London, 1974), pp. 163-199. The numerical fitting algorithms used in the ODP, including singular value decomposition, are discussed by C. L. Lawson and R. J. Hanson, *Solving Least Squares Problems*, (Prentice Hall, Englewood Cliffs, NJ, 1974).
9. Currently accepted astronomical constants and reference systems are given in P. K. Seidelmann, Ed., *Explanatory Supplement to the Astronomical Almanac* (University Science Books, Mill Valley, CA, 1992).
10. A Celestial Mechanics Experiment, similar to the Galileo experiment discussed here, was included on the Pioneer 10 and 11 Missions, but not on the Voyager Mission at Jupiter. Prior to the Galileo Mission, the best information on the Jupiter gravity field was provided by Pioneer 11 at a flyby distance of 113,000 km (1.61  $R_J$ ). However, the Pioneer 11 experiment was limited by the occultation of the spacecraft by Jupiter at closest approach. Results were reported by G. W. Null, J. D. Anderson, S. K.

Wong, *Science* 12, 476-477 (1975), J. D. Anderson in *Jupiter*, T. Gehrels, Ed. (The Univ. of Arizona Press, Tucson, AZ, 1976), pp. 113-121, G. W. Null, *Astron. Jour.* 81, 1153-1161 (1976). After Voyager 1 and Voyager 2 completed their Jupiter flybys, J. K. Campbell and S. P. Synnott, *Astron. Jour.* 90, 364-372 (1985) combined the Pioneer 10 and 11 Doppler data with Voyager navigation data to obtain the most comprehensive information on the gravity field of the entire jovian system. Because of data limitations and the nature of the four flybys they considered, they had the most difficulty determining GM values for Io, Europa, and the Jupiter system, the three parameters most accessible with the Galileo data. In GM units of  $\text{km}^3 \text{s}^{-2}$ , their formal uncertainties (as derived from the least-squares covariance matrix) were unity for both Io and Europa, and only 5 on the system GM. However, to compensate for systematic errors and to report what they considered realistic standard errors, they increased these GM errors to 10 for Io and Europa, and to 100 for the system. Our recommended Galileo standard errors are considerably smaller than prior realistic errors. This improvement results from the close Galileo flybys of Io and Europa. The Galileo Europa flyby at 32,958 km contrasts with the closest prior flyby by Voyager 2 at 206,000 km. Similarly, the Galileo Io flyby at 2718 km contrasts with the Voyager 1 flyby at 21,000 km. The Galileo Jupiter flyby at a distance of 214,574 km ( $3.05 R_J$ ) is comparable to Pioneer 10 at 203,000 km. The Voyager 1 and 2 flybys were more distant at 349,000 and 722,000 km, respectively.

11. B. D. Tapley in *Recent Advances in Dynamical Astronomy*, B. D. Tapley and V. Szebehely, Eds. (D. Reidel, Dordrecht and Boston, MA, 1973), pp. 396-425 discusses the

statistics of orbit determination, including the linearization of the nonlinear problem, and the minimum variance estimate with a priori information - two techniques used in our analysis.

12. R. A. Jacobson of JPL, developed new satellite ephemerides for the Galileo Project in support of the Navigation Team. He numerically integrated the four Galilean satellites and fit ground-based astrometric data, including satellite mutual events. His force model included the best available Jupiter gravity parameters (10). He included 33 parameters in the fit, including the initial position and velocity for the four Galilean satellites, five GM values for the satellites and the Jupiter system,  $J_2$  and  $J_4$  for Jupiter, and the right ascension and declination of Jupiter's pole. He made small corrections to the five GM values, but left the Jupiter gravity parameters and the pole unchanged from their spacecraft flyby values. The fitting model was fully relativistic, consistent with the ODP. Relativistic terms in the satellite orbits are important for consistency, but they are too small to provide tests of general relativity.
13. This arcane terminology from classical celestial mechanics can be found in standard texts on the subject, for example, F. R. Moulton, *An introduction to Celestial Mechanics* (Macmillan, New York, ed. 2, 1914), or at a more advanced level, D. Brouwer and G. M. Clemence, *Methods of Celestial Mechanics* (Academic Press, New York, 1961). The radius  $r$  depends on the true anomaly  $f$  through the polar equation of a conic section centered at one focus;  $r = p/(1 + e \cos f)$ , where  $p$  is the semi-latus rectum and  $e$  is the eccentricity.
14. Formal error estimates from the least-squares covariance matrix are based on an as-



sumption of independent measurements drawn from a Gaussian noise distribution. The Galileo Doppler frequency data are Gaussian, but their power spectral density follows an  $f^{-2/3}$  law arising from propagation of the radio carrier wave through solar plasma (Fig. 2). R. Woo and J. W. Armstrong, *Jour. Geophys. Res.* 84, 7288-7296 (1979) have shown that this is the expected noise spectrum for a radio wave passing more than 20 solar radii ( $5.5^\circ$ ) from the Sun and subject to a one dimensional Kolmogorov electron density spectrum with spectral index 5/3. The variance of spectral estimates of a signal roughly follows the same power law dependence as the noise spectrum, so the Galileo gravity signals are better determined at higher Fourier frequencies. Our data weighting, with an assumed variance approximately equal to the variance of the Doppler residuals ( $4 \text{ mm}^2 \text{ s}^{-2}$ ), is about right for the Io and Europa gravity signals, where the peak Fourier components are around  $2 \times 10^{-3} \text{ Hz}$ . However, it is too optimistic for the lower-frequency Jupiter mass signal. We therefore retain the formal errors for the satellite gravity parameters, but increase the formal Jupiter mass error by a factor of three. All errors reported in this article are best estimates of realistic standard error,

15. E. R. Cohen and B. N. Taylor, *Rev. Mod. Phys.* 57, 1121-1148 (1987). The currently accepted value of  $G$  has been challenged by experimental groups engaged in new laboratory measurements (see the report in *Science News*: 4/29/95, p.263). If a new value for  $G$  is adopted by the physics community, a revision of the masses reported here may be necessary. The mass is determined from the flyby values of  $GM$  divided by  $G$ , so a fractional change in  $G$  would require the same fractional change in the mass with oppo-

site sign. The current mean densities for 10 and Europa are limited by the uncertainty in  $G$  and by current uncertainties in satellite volumes. As the Galileo Orbital Mission progresses, improved volumes should become available from imaging data analysis.

16. In deriving the mass of the Sun to the mass of a planet, a value of  $GM_{\odot} = 1.327124408 \times 10^{21} \text{ km}^3 \text{ S}^{-2}$  is used. It is the best determined constant in astronomy and is accurate to the number of digits given. It is determined from accurately known periods of the planets together with radio ranging measurements between Earth and Mars with Viking Landers between 1976 and 1982; see R. D. Reasenberg *et al.*, *Astrophys. J.* 234, 1,219 (1979); The *Astronomical Almanac for the Year 1988* (Government Printing Office, Washington DC, 1987); A. M. Nobili and C. M. Will, *Nature* 320,39 (1986).
17. M. Segatz, T. Spohn, M. N. Ross, G. Schubert, *Icarus* 75, 187-206 (1988); M. Wienbruch and T. Spohn, *Planet. Space Science* 43, 1045-1057 (1995).
18. M. Davies *et al.*, *Celest. Mech. and Dyn. Astron.* 53, 377-397 (1992) give values for the three principal axes of 10 as determined by Voyager 1 imaging data. The axes are  $a=1830.0 \text{ km}$ ,  $b=1818.7 \text{ km}$ , and  $c=1815.3 \text{ km}$ , all with uncertainties of 0.2 km. The error characteristics of an elliptical shape determination can be derived from an assumed continuous distribution of radius measurements. For the flattening  $(a-c)/c$ , the error is equal to  $\sqrt{8}$  times the fractional error in each independent radius measurement (we assume 0.2/1821 for 10). Using the published axes and this error result, we obtain  $(a-c)/c = (8.10 \pm 0.31) \times 10^{-3}$  and  $(b-c)/c = (1.87 \pm 0.31) \times 10^{-3}$ . These values and their estimated uncertainties are consistent with Table 2.

19. This experiment was coordinated at JPL, by the Galileo Radio Science Support Team, IL G. Herrera Team Leader. The radio Doppler data were generated with the support of the Office of Tracking and Data Acquisition and the Deep Space Network. The data analysis depended on the availability of software and personnel of the Galileo Project Navigation Team, W. E. Kirhofer Team Leader. We thank all concerned for their help and advice. We also thank E. L. Lau for generating plots from ODP computer files. This work was sponsored by the Galileo Project and was performed at the Jet Propulsion Laboratory, California Institute of Technology, under contract with the National Aeronautics and Space Administration,

## 6 Figure Legends

Fig. 1. Plot of the  $C_{22}$  10 gravity signal (solid line) detected in the noncoherent Doppler data near 10 closest approach. Noncoherent data are referenced to the spacecraft's temperature-controlled crystal oscillator (USO). Units of Doppler frequency shift are  $\text{mm s}^{-1}$  according to the formula  $c\Delta\nu/\nu$ . Here  $\text{AU}$  represents the Doppler frequency shift in  $\text{Hz}$ ,  $\nu = 2.3 \times 10^9 \text{ Hz}$  is approximately the spacecraft's S-band transmitter frequency, and the speed of light  $c = 2.998 \times 10^{11} \text{ mm s}^{-1}$ . The dashed lines represent the  $\pm 2 \text{ mm s}^{-1}$  standard error of the data. The bias in the signal after closest approach versus before closest approach is masked by other parameters in the fit. It is the rapidly changing gravity signal on a time scale of 20 min that yields the parameter  $C_{22}$ .

Fig. 2. Estimate of power- spectral density for combined coherent and noncoherent

Doppler frequency residuals. The dashed line represents  $f^{-2/3}$  solar plasma noise (14). All significant systematic trends have been removed by the 23-parameter fit. The increase in the spectrum at about  $2 \times 10^{-4}$  Hz (5000 s period), and decrease at lower frequencies, is a result of statistical nonstationarity over the 3.8 days of the experiment. The variance on the residuals, equal to the integral of the spectrum over the entire bandwidth of the data, is  $6.455 \text{ mm}^2 \text{ s}^{-2}$  and the corresponding standard error is  $2.54 \text{ mm s}^{-1}$ . In a narrower high-frequency band starting at the lower limit for the 10 gravity signal at about  $2.78 \times 10^{-4}$  Hz (3600 s period), and extending to the high-frequency cutoff, the standard error is  $2.17 \text{ mm s}^{-1}$ . The data weights used in the least-squares data analysis described in the text correspond to a standard error of  $2 \text{ mm s}^{-1}$  at a 60 s sample interval. This weighting yields a realistic estimate of the error for the 10 and Europa gravity parameters, but for lower-frequency components, such as the Jupiter mass signal, it underestimates the realistic error by a factor of three.

Fig. 3. Ratio of core radius to 10 radius (a) and core mass fraction (b) versus ratio of core density to mean density  $\rho_c/\bar{\rho}$  with  $C_{22}$  as a parameter. The ratio  $\rho_c/\bar{\rho}$  is assumed to vary between 1.46 and 2.29. These extreme values correspond to  $\rho_c = 5150$  and  $8090 \text{ kg m}^{-3}$ , the densities of an Fe-FeS eutectic composition core and a pure Fe core, respectively (17).

## 7 Tables

**Table 1.** Initial Galileo gravity results compared to  
previous Pioneer and Voyager results (10)

GM units are  $\text{km}^3 \text{S}^{-2}$ ; units  $10^{-6}$  for gravity coefficients  $C_{22}, J_2, J_4, J_6$

Parameter	Galileo	Pioneer and Voyager
$C_{22}(\text{Io})$	5 5 9 3 2 7	None
GM (System)	126,712,752 $\pm$ 40	126,712,767 $\pm$ 100
GM (Jupiter)	126,686,527 $\pm$ 40	126,686,537 $\pm$ 100
GM (Io)	5959.91 $\pm$ 0.28	5961 $\pm$ 10
GM (Europa)	3196.81 $\pm$ 0.69	3200 $\pm$ 10
GM (Ganymede)	None	9887 $\pm$ 3
GM (Callisto)	None	7181 $\pm$ 3
$J_2$ (Jupiter)	None	14736 $\pm$ 1
$J_4$ (Jupiter)	None	-587 $\pm$ 5
$J_6$ (Jupiter)	None	31 $\pm$ 20

**Table 2.** Two layer 10 models for inferred values of  $C_{22}$ .

$\rho_c/\bar{\rho} = 1.459$  for FeFeS core model and 2.292 for Fe core model.

$C_{22}$ units $10^{-26}$	<i>532</i>	<i>559</i>	<i>586</i>
$C/MR^2$	<i>0.371</i>	<i>0.378</i>	<i>0.386</i>
$(a - c)/c$ units $10^{-3}$	<i>7.681</i>	<i>7.897</i>	<i>8.113</i>
$(b - c)/c$ units $10^{-3}$	<i>1.920</i>	<i>1.974</i>	<i>2.028</i>
FeFeS core model			
$r_c/R$	0.576	0.517	0.447
MC/M	0.279	0.202	0.130
Fe core model]			
$r_c/R$	0.397	0.357	0.310
MC/M	0.143	0.105	0.068

Fig. 1

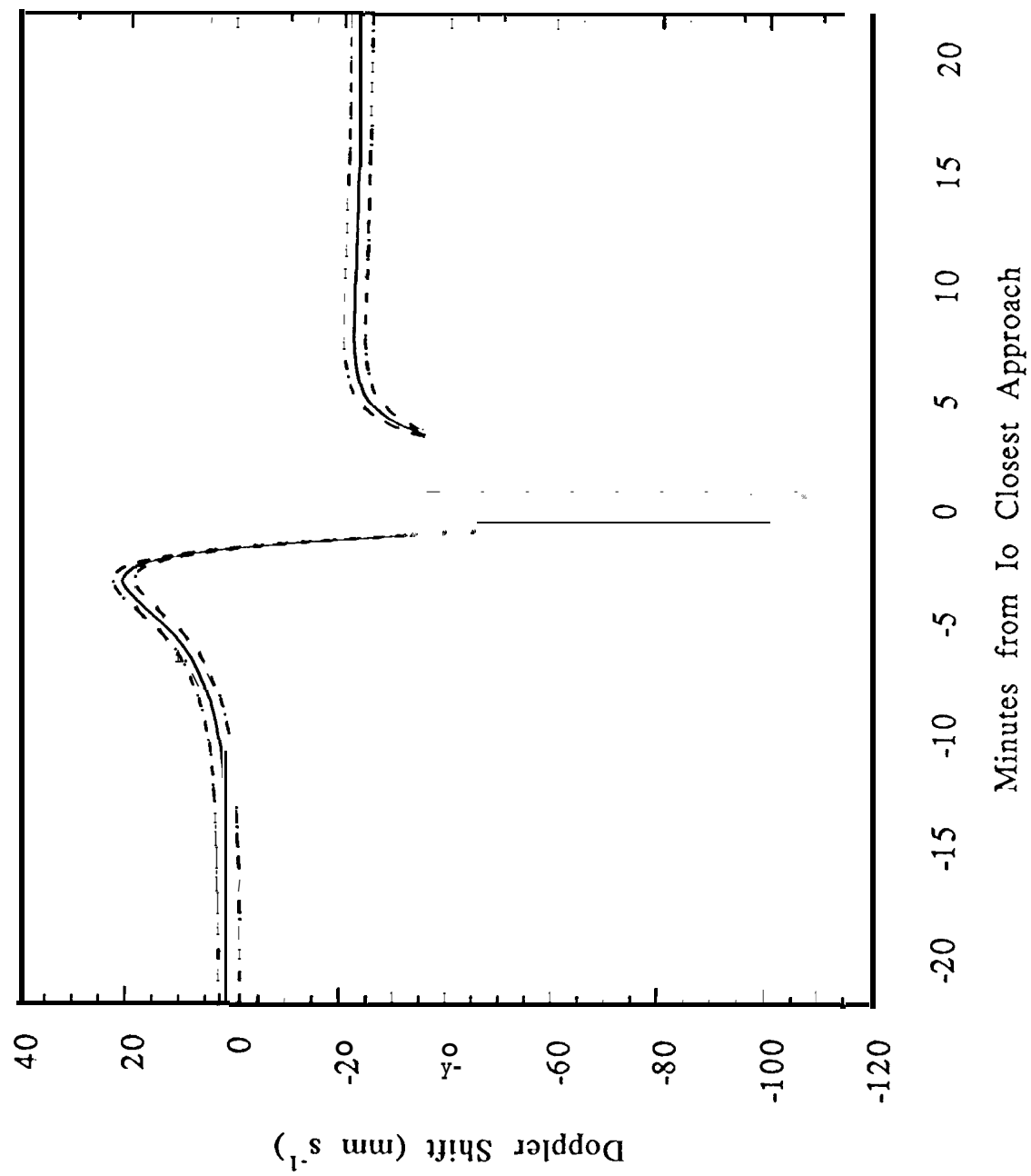


Fig. 2

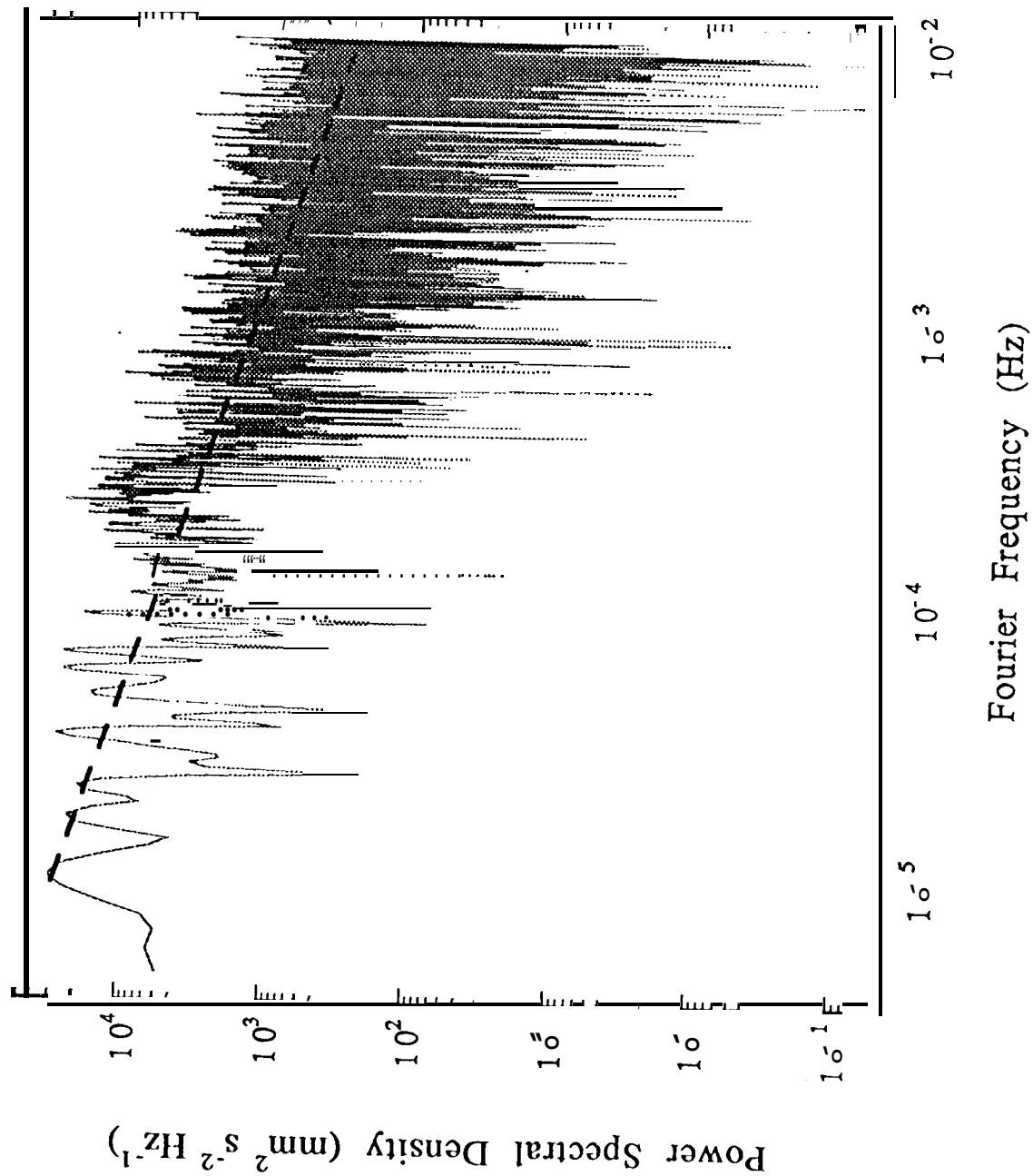




Fig. 3a.

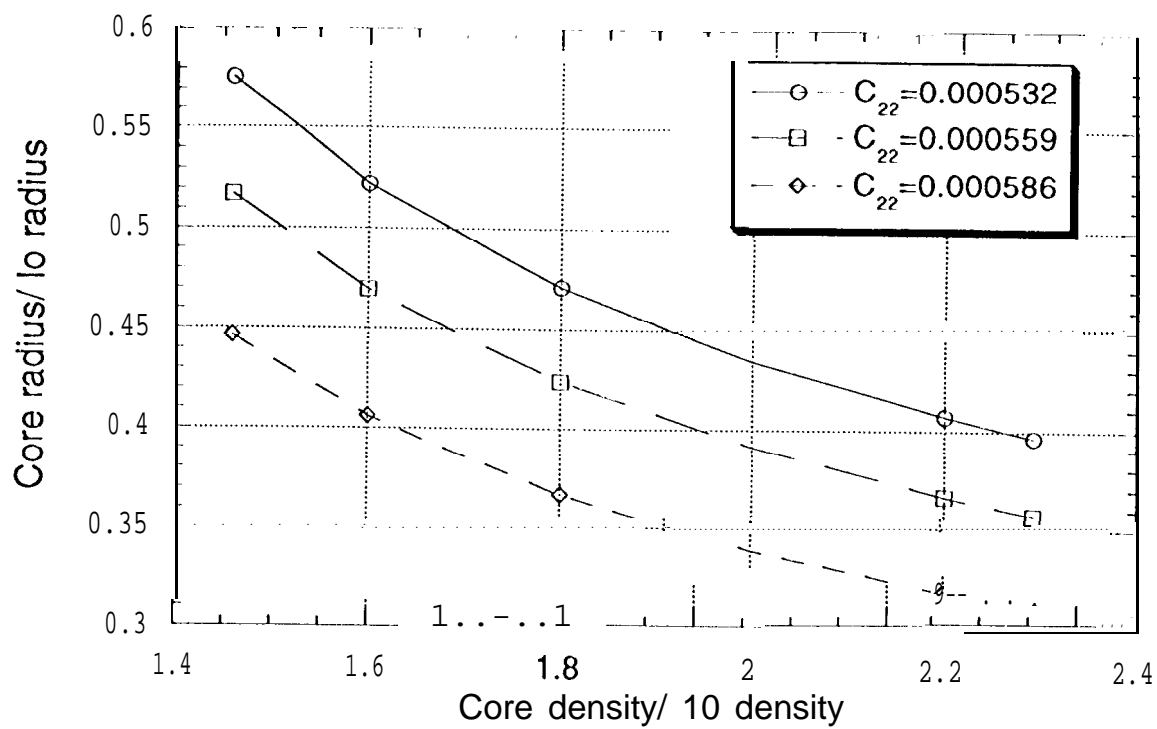


Fig. 36

